Arabian Journal for Science and Engineering
https://doi.org/10.1007/s13369-024-09170-8

RESEARCH ARTICLE-MECHANICAL ENGINEERING

Influence of the Heated-Bed Material on PLA Mechanical Properties and Energy Consumption in the FDM Process

Ersilia Cozzolino[1] · Francesco Napolitano[1] · Ilaria Papa[1] · Antonino Squillace[1] · Antonello Astarita[1]

Received: 20 November 2023 / Accepted: 9 May 2024

Abstract
Among the different investigations carried out on polymer additive manufacturing, the influence of the plate material is often neglected. The energy-saving perspective forces us to study the improvement of the 3D printer architecture to optimize the process conditions by minimizing power and energy consumption. This research moves from the intent to preserve the part quality and avoid energy dissipation in the 3D printer plate. This component requires the most energy input to work properly and it is also in direct contact with the workpiece, resulting in paramount for the lower layers. By analyzing a previously assessed set of process parameters, three plate materials were adopted and investigated in this study. Tensile and ultrasonic tests were carried out to evaluate the PLA specimen's quality and mechanical performance: Both gave good results proving the poor influence of the metallic plate on the workpiece. The results obtained in this experimental study allowed to release of some guidelines for better decision-making in the choice of a material plate for desktop 3D printers to print PLA from a sustainable perspective. The best results have been observed by selecting $V = 110$ mm/s and $T = 215$ °C as process conditions by using the aluminum plate. Also, the ultrasound analysis confirms greater uniformity of the material at a printing speed $V = 110$ mm/s for all the printing plates indicating a low influence of the printing plates used on the material uniformity.

Keywords PLA · FDM · Additive manufacturing · Sustainability · Energy consumption · Mechanical properties

1 Introduction

Additive manufacturing (AM) is a potentially valuable solution for addressing lightweighting needs, as it takes advantage of the design freedoms offered by material complexity principles. AM technologies are recognized for their environmental friendliness, as they use only the necessary amount of material for the product [1]. Additionally, AM methods can reduce life cycle material mass and energy consumption compared to traditional subtractive processes by minimizing scrap. Certain AM methods enable the repair and remanufacturing of defective tools, which can eliminate the need for supply chain processes associated with creating new tooling [2]. Furthermore, it has been demonstrated by life cycle assessment (LCA) that the implementation of AM can lead to substantial savings during both the manufacturing and usage phases of a product's life cycle. These savings are achieved by shortening the time between design and production and by optimizing component form to fully utilize AM capabilities, resulting in additional cost savings [3]. Moreover, as reported by several studies, AM can significantly reduce energy consumption and emissions through lightweight design optimization [4, 5].

Currently, the large use of desktop 3D printers establishes some issues by considering the environmental impact of home activities. A sustainability perspective suggests developing new ways for 3D printing parts in an energy-saving approach. In a previous research study, it was observed that the greatest contribution in terms of energy consumption is given by the heating of the plate and the continuous cycles to keep it warm [6]. As a matter of fact, the power spent to heat the plate is at least 60% of the total power demanded by the machine and, for the conventional plate made by steel, the thermal dispersion forces the system to keep the power on for the whole printing cycle because the bed has difficulties to reach the target value in particular when it is too high with respect to the room temperature.

✉ Francesco Napolitano
francesco.napolitano4@unina.it

[1] Department of Chemical, Materials and Industrial Production Engineering, University of Naples "Federico II", P.le Tecchio 80, 80125 Naples, Italy

Published online: 27 May 2024

In this scenario, the redesign of the plate was considered crucial to pursue the energy consumption reduction on large-scale device use. By considering new base material to be employed in plate manufacturing, different alternatives were chosen to enhance some thermal aspects while paying particular attention to the dimensional stability. The first aspect which was evaluated regards the thermal characteristics because the time required to warm up the plate is too long in case of steel therefore the choice includes the Aluminum alloy 2024 which has 8 times the thermal conductivity respect to the steel (aluminum 193 W/m–K–steel 24.9 W/m–K) and double specific heat capacity (aluminum 0.875 J/g-K–steel 0.46 J/g-K). On the opposite side was considered a material with a low thermal conductivity and specific heat capacity comparable to the steel so having high thermal inertia, a Nickel based superalloy nimonic 75 (13.4 W/m–K and 0.461 J/g-K). The first one could ensure rapid heating of the plate which results in energy consumption reduction obtained through the reduction of the heating time, on the other hand it could require more on/off cycles that generate a continuous increase and decrease in the adsorbed power. The second material could require too long heating time and then too high energy consumption in the warm-up phase, but it could offer more stability in keeping the temperature high and as consequence the increase in initial energy consumption caused by the increase in time required for the heating phase but more stability in keep the temperature level avoiding a large number of on/off cycles.

As regards the plate, the main topic investigated in the literature is the influence of the plate temperature on the mechanical properties of the printed components [7–9] and its influence on different extruded materials [10–13]. Table 1 contains the main recent works on the research topic of this study. In other works, the plate shrinkage and the correlation with the workpiece dimensional accuracy were evaluated [14]. Also, the possibility to use a new material for the plate was investigated with the aim to improve the mechanical properties [15]. In any case, each optimization was not related to the energy consumption evaluation and the influence of the plate material on the mechanical properties was neglected, and therefore the purpose of this research work is to optimize the energy consumption by preserving the mechanical properties.

Lepoivre et al. discussed heat transfer model and the adhesion by considering the temperature of the plate independently from the material of the plate [16]. The interest in heat transfer is proven by different studies which correlate different numerical models and experimental results [17, 18]. The heat transfer mechanism and its influence on the filament adhesion were also studied by directly monitoring the workpiece during the printing [19, 20].

On this basis, the experimental study was carried out considering the steel standard plate as a reference and the other

Table 1 Recent related works on the research topic of this study

References	Process	Material	Properties investigated
Peng et al. [8]	FDM	CF/PA6	Tensile strength
Luzanin et al. [9]	FDM	PLA	Tensile strength, crystallinity, mesostructure
Mostafa et al. [10]	FDM	Nylon 12	Tensile strength
Khabia et al. [11]	FDM	ABS	Tensile strength, elongation at break
Lay et al. [12]	FDM	PLA, ABS and Nylon 6	Crystallinity, tensile strength, elongation at break, impact strength
Agarwal et al. [13]	FDM	ABS	Dimensional accuracy
Choi et al. [14]	FDM	ABS	Heat shrink shape errors
Messimer et al. [15]	FDM	ABS, PLA, PET, HIPS, PC, TPU, PVA, nylon, metal PLA, and carbon-fiber PLA	Printability by varying the material bedplate (AL–glass and AL-PC)
Lepoivre et al. [16]	FFF	ABS, PEKK	Heat transfer and the adhesion behavior
Kousiatza et al. [17]	FDM	ABS	In situ and in real-time temperature development within multilayered square thin plates
Prajapati et al. [19]	FDM	ABS	Temperature distribution on the build plate
Roy et al. [20]	FFF	ABS	Temperature effect on the functional properties of the parts

Table 2 Experimental plan of PLA samples manufactured by FFF: the fixed process parameters

Infill percentage	100%
Layer height	0.2 mm
Orientation	− 45°/ + 45°
Pattern	Line infill
Plate temperature	90 °C
Number of shells	2

plates for the investigation of the specific thermal property. Since PolyLacticid (PLA) is a material widely used in polymeric AM, the experimentation was based on the printing monitoring of this material for ease of execution given the wide knowledge of the process parameters useful for the printability of the treated material. In this regard, the heat input quantity required to print tensile and square samples was analyzed in terms of power adsorbed to evaluate the energy consumption. Finally the results of the ultrasonic inspections and the tensile tests, performed on each sample, were used to correlate the heat transfer mode and the mechanical properties of the printed pieces. All the considerations were connected to be examined from the perspective of sustainable manufacturing.

Table 3 Experimental plan of PLA samples manufactured by FFF: the varied process parameters

Configuration	Plate material	Speed (mm/s)	Extrusion temperature (°C)
1	AISI 430 stainless steel	70	215
2	AISI 430 stainless steel	110	215 (1st–7th layers) 230 (8th–15th layers)
1	2024 Aluminum	70	215
2	2024 Aluminum	110	215 (1st–7th layers) 230 (8th–15th layers)
1	Nimonic	70	215
2	Nimonic	110	215 (1st–7th layers) 230 (8th–15th layers)

2 Materials and Methods

2.1 FDM Process

Among all the AM techniques, the most common is fused filament fabrication (FFF) that is a 3D printing process that uses a continuous filament of a thermoplastic material and it is a cost-effective, almost-zero-waste, and user-friendly approach [21, 22] Square samples 50 × 50 × 3 mm were printed by the fused filament fabrication (FFF) technique by means of Sharebot 42, which is 450 × 420 × 470 mm in size and has a printing volume of 250 × 220 × 220 mm. The samples were firstly designed into Solidworks software and then sliced by Simplify 3D software, where the printing was simulated after fixing the process parameters. Black PLA ICE Filaments having a diameter of 1.75 mm were used for printing the samples. Infill percentage, layer height, orientation, pattern, plate temperature, and number of shells were fixed for all the samples as expressed in Table 1. Conversely, extruder temperature and deposition speed were varied for all the samples. The fixed process parameters for all the samples are expressed in Table 2. They were chosen according to the best results in the literature [23, 24].

Based on the best results in terms of both the energy consumption and mechanical properties [23–26], two temperature strategies combined with two levels of deposition speed were chosen for our experimental campaign as contained in Table 3. All the configurations of PLA samples were printed by using three plates as building platforms, having the same geometrical features and different materials, that are AISI 430 stainless Steel, 2024 Aluminum, nimonic.

In this study, after the 3D printing of PLA samples, tensile tests, ultrasonic inspection, and an energy consumption analysis have been carried out.

2.2 Energy Consumption

The device Quality Analyzer CA8331 was used to measure power and energy consumption during the FDM process by means of current and tension measurements. It is a high-quality analyzer with a color and battery graphic display built-in rechargeable, that is equipped with four tension cables, four crocodile clips and three current sensors Mini-FLEX MA193-350. The electrical system of the 3D printer consists of a mono-phase with neutral cable 10 A 250 V. The current and tension sensors are connected to an intermediary electrical system—the single phase and the neutral—between the electrical cabinet and the cable connection of the 3D printer. The experimental setup is schematically displayed in Fig. 1. A sampling period of one second has been chosen to measure power and energy consumption over time.

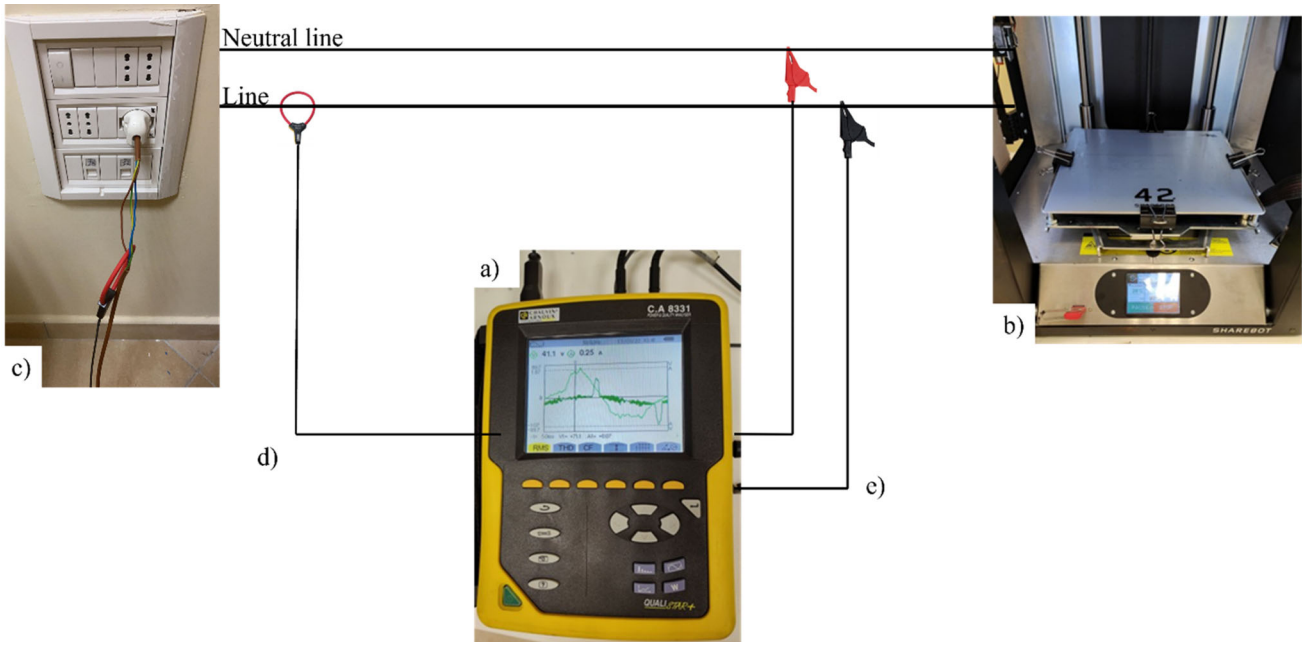

Fig. 1 Experimental setup: **a** the power and the energy analyzer, **b** the 3D printer, **c** the electrical cabinet, **d** the current sensor, **e** the tension cables (Experimental integrated approach for mechanical characteristic optimization of FDM-printed PLA in an energy-saving perspective [6])

The mass of each sample was measured three times by means of Gibertini ETERNITY 200 CAL balance, which has an accuracy of ± 0.05 mg. These measurements have allowed calculating the specific energy consumption (SEC), which is highly used in the literature as a key sustainable performance indicator [27]. In the FDM process, SEC (kJ/g) represents the energy consumption for printing the mass unit and is expressed as follows:

$$\mathrm{SEC} = E_{\mathrm{print}}/m \tag{1}$$

where E_{print} is the energy consumption for printing the single sample, and m is the mass of the sample.

2.3 Tensile Tests

Uniaxial tensile tests were carried out to investigate the mechanical properties of the samples by means of a Galdabini QUASAR 50 testing machine. It is equipped with a 50 kN load cell and a micron extensometer that allows to measure the deformation up to the rupture. The tests were performed at room temperature and at a speed equal to 3 mm/min. LabTest is the software associated with the Galdabini machine that allows programming the tests according to the ASTM International Standards [28]. Thus, to evaluate the tensile strength, three tensile specimens with the ASTM standard geometry were printed for each combination of process conditions, as defined in Subsect. 2.1.

2.4 Ultrasonic Inspection

A US Multi2000 Pocket 16 × 64 instrument was used to carry out ultrasound inspection to evaluate the goodness of the printed samples in terms of compaction and homogeneity. A single Probe, DS 6 HB 2–7 made by KARL DEUTSCH, 5 MHz was applied to have a good signal acquisition and reduce its attenuation as previously used in previous studies [6].

The pulse-echo technique was used for the quality internal detection of the components. Short-duration ultrasonic pulses were transmitted into the all regions, and the echo signals—caused by wave scattering and reflection—were detected and displayed. The depth of a reflective structure is inferred from the delay between pulse transmission and echo reception. Using this method on an undamaged sample, the correct plate thickness is obtained and the acquisition system is calibrated. The propagation velocity through the material, equal to 1200 mm/s, was set [6].

The inspection of the material has been carried out analyzing the A scan visual that is a reconstruction of the ultrasound signal's travel in the inspected material. It consists of a series of peaks, the position of which along the horizontal axis can be calibrated in terms of the depth in the material. The amplitude, A, of each echo will give some indication of the size and nature of reflector, which might be a flaw or a specimen boundary.

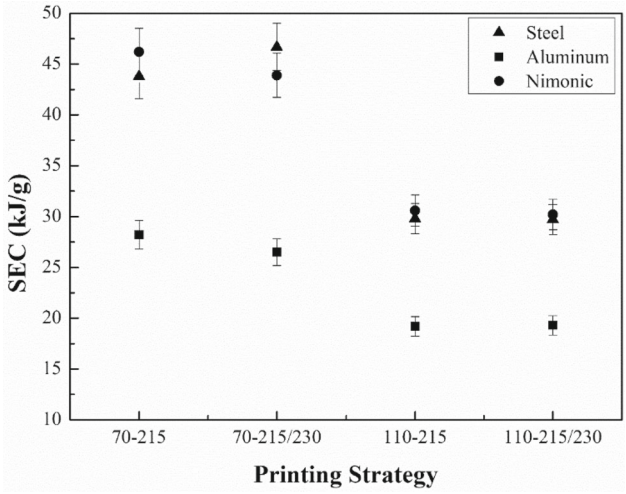

Fig. 2 SEC vs printing strategy for each bed surface

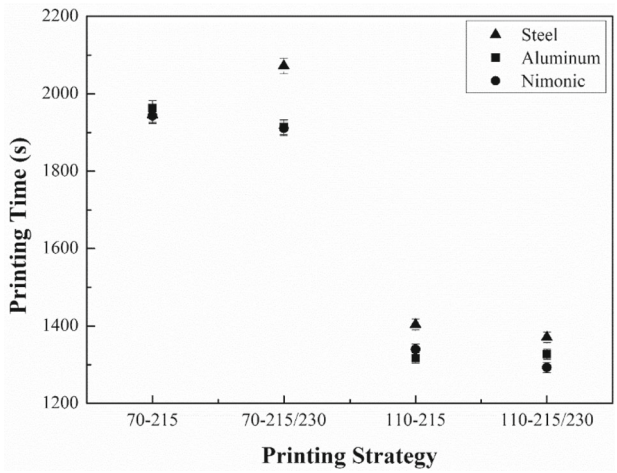

Fig. 3 Printing time versus printing strategy for each bed surface-plate material

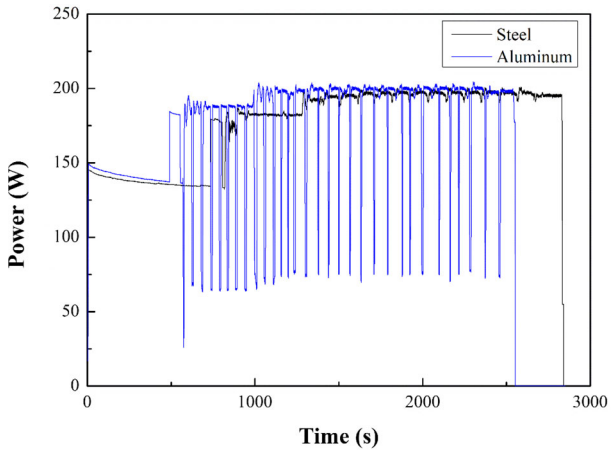

Fig. 4 Power signal for printing strategy 215 °C–70 mm/s

3 Results and Discussion

As previously mentioned, the influence of the plate material in the FDM process is often neglected in the literature. Peng et al. [8] investigated the effects of processing parameters during FDM printing on mechanical properties and interlayer adhesion tensile properties of carbon-fiber reinforced polyamide 6 (CF/PA6). In their study, build-plate temperatures were found to own a close relationship with the tensile properties and interlayer adhesion. Also, they found that strength and modulus of FDM-printed CF/PA6 specimens continuously increase with decreased voids (porosity) as the build-plate temperature increases. Luzanin et al. [9] investigated the impact of layer thickness, extrusion temperature, extrusion speed and build-plate temperature on the tensile strength, crystallinity achieved during fabrication and mesostructure of PLA specimens. They found that layer thickness and its quadratic effect are dominant contributors to tensile strength. Significant interaction between layer thickness and extrusion speed implies that these parameters should always be varied simultaneously within designed experiment to obtain adequate process model. Thus, a lot of studies in the literature only take into account the part quality as objective of the FDM process optimization [8–14]. Very few studies in the literature investigate the temperature distribution during the FDM process, and just a very small part of them consider the minimization of the energy consumption during the printing among the objectives [15–20]. In this regard, this experimental study aims to fill this gap of knowledge. In fact, the energy-saving perspective, which leads the production sectors today, forces to study the improvement of the 3D printer architecture in order to optimize the process conditions by minimizing power and energy consumption. In the following sections energy consumption analysis, tensile tests and ultrasonic inspection are presented. Thus, the influence of the heated-bed material on PLA mechanical properties and energy consumption in the FDM process.

3.1 Energy Consumption

The values resulting from the energy consumption analysis are reported in the table below (Table 3). Figure 2 shows how the specific energy consumption (SEC), expressed in Eq. (1), varies by selecting a different printing strategy referring to the different extrusion temperature by using different plate materials, as above discussed. Similarly, Fig. 3 depicts the printing time by varying the printing strategy. It is relevant to note that the printing time is the most important index of sustainability, as a matter of fact the printing strategies with the highest nozzle speed have the lowest SEC independently from the bedplate material. Thus, as observable from Figs. 2 and 3, there is a linear correlation between the SEC and the

Table 4 Energy consumption analysis results

Bed material	Print speed (mm/s)	T extrusion (°C)	E_p(kJ)	Weight (g)	SEC (kJ/g)	Printing time (s)
Steel	70	215	381.6	8.71	43.8	1946
		215/230	403.2	8.63	46.7	2072
	110	215	255.6	8.59	29.8	1404
		215/230	259.2	8.73	29.7	1371
Aluminum	70	215	259.4	9.21	28.2	1963
		215/230	244.8	9.23	26.5	1914
	110	215	175.8	9.18	19.2	1317
		215/230	176.4	9.15	19.3	1327
Nimonic	70	215	409.8	8.87	46.2	1943
		215/230	381.2	8.68	43.9	1911
	110	215	270.2	8.82	30.6	1340
		215/230	268.8	8.80	30.2	1293

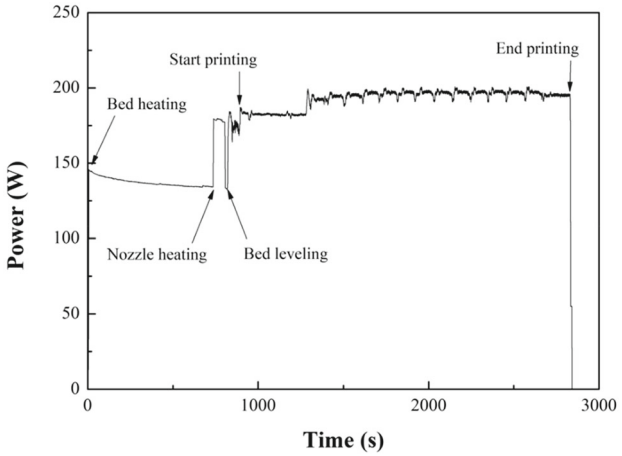

Fig. 5 Segment identification on the power consumption curve (printing strategy 215 °C–70 mm/s) using the steel plate

printing time, as expected [6]. Table 4 contains the results of the energy consumption analysis.

Since the performance indexes and the acquired power signals for the steel bedplate and the nimonic bedplate are shown to be very similar to each other, the only power signal during the printing on the steel plate has been compared with that on the aluminum one to highlight the differences in the bedplate behavior (Fig. 4). Two differences immediately appear, the bed heating segment is very short with the aluminum plate setup than the steel, during the printing phase, there are a lot of on/off occurrences in the aluminum curve that are related to the bedplate heating. They could be better understood by observing the identification of the curve segments in Fig. 5.

The weight of power consumption on the process productivity has been better analyzed by evaluating the energy required in each single phase of the printing process.

The pie charts reported in Fig. 6 show a decrease in the bed heating contribution and an increase up to 77% of the energy spent for the printing phase, which is the only value-added phase because just in this phase, the workpiece is built. The same behavior is reported in phase duration pie charts, the rapid heating of the aluminum bedplate allows the increase of the time percentage spent to print the component (Fig. 7). Nevertheless, the printing time is independent from the capacity to reach and to keep the target temperature, because it depends just on the nozzle speed. So, the significative differences reported by the energy spent are even more important since it means that, although the duration of each phase does not change, the energy spent is improved. The last is due to the numerous on/off heating cycles during the printing phase (Fig. 4). This phenomenon indicates that the 3D printer continuously requires energy to keep the steel plate at 90 °C, differently from the aluminum plate, according to their different thermal properties. As a result, it has been reported that the aluminum bedplate gives the lowest SEC for each printing condition (Table 3). These values are even lower than the values given by the other two bedplate material, because of his highest thermal conductivity among those of the bedplate materials adopted in this study. In fact, aluminum alloy 2024 has a thermal conductivity of 193 W/m–K, steel has a thermal conductivity of 24.9 W/m–K whereas nimonic has a thermal conductivity of 13.4 W/m–K. Thus, it is better to use aluminum plates for the desktop 3D printers rather than steel plates to reduce power and energy consumption of the FDM process.

3.2 Tensile Tests

As explained in Subsect. 2.3, three tensile specimens have been printed and tested for each printing strategy. Table 5

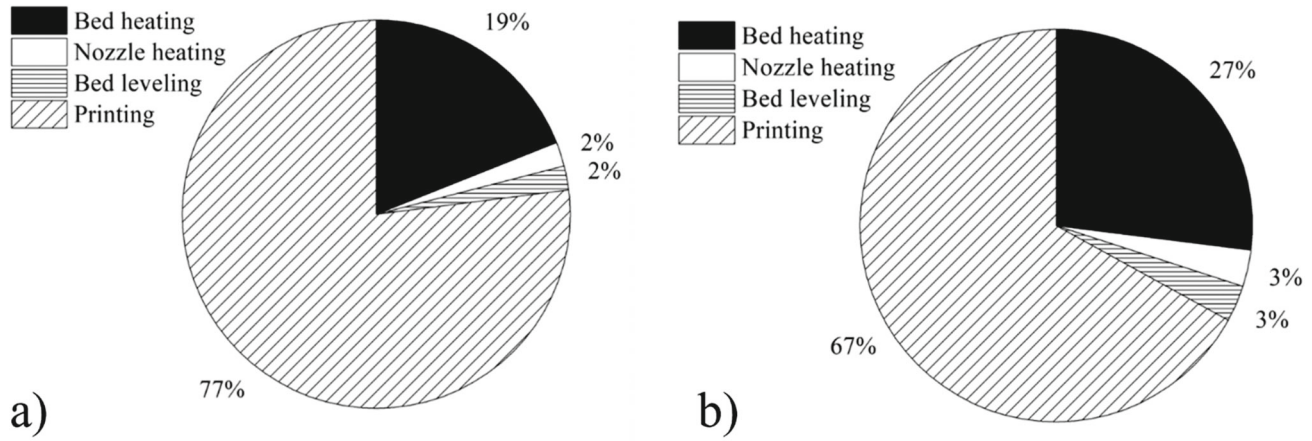

Fig. 6 Contribution of the energy spent during the different phases of the printing process by using the **a** aluminum bedplate and the **b** steel bedplate

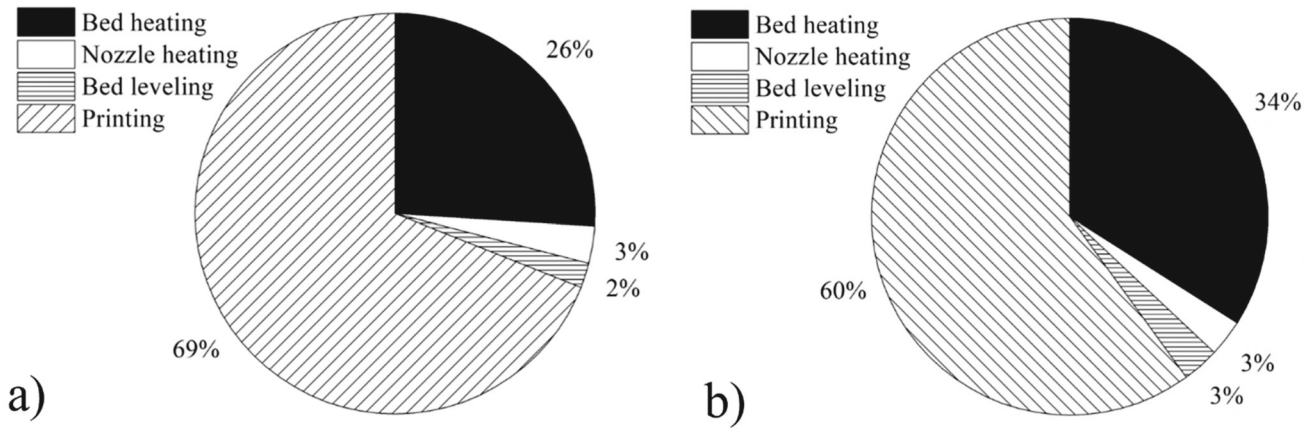

Fig. 7 Time duration of the different phases of the printing process by using the **a** aluminum bedplate and the **b** steel bedplate

Table 5 Tensile test results

Bed material	Print speed (mm/s)	*T* extrusion (°C)	UTS (MPa)	SEC (kJ/g)	UTS/SEC
Steel	70	215	44.5	43.8	1.0
		215/230	50.1	46.7	1.1
	110	215	50.6	29.8	1.7
		215/230	45.4	29.7	1.5
Aluminum	70	215	44.5	28.2	1.6
		215/230	44.6	26.5	1.7
	110	215	50.6	19.2	2.6
		215/230	45.4	19.3	2.4
Nimonic	70	215	40.0	46.2	0.9
		215/230	46.0	43.9	1.0
	110	215	45.7	30.6	1.5
		215/230	41.0	30.2	1.4

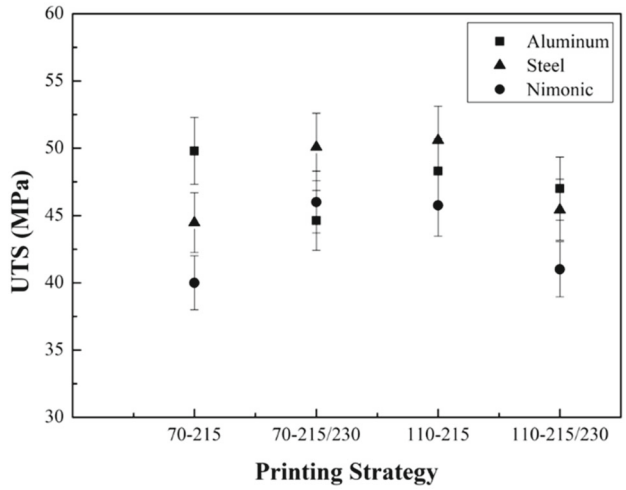

Fig. 8 UTS versus the printing strategies adopted in this study

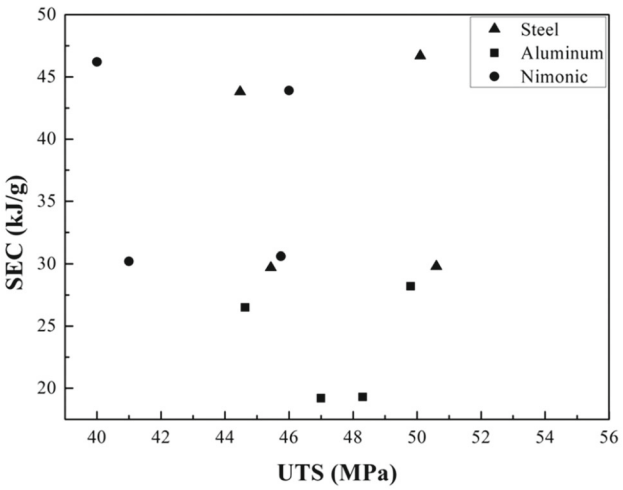

Fig. 9 SEC versus UTS of all the strategies adopted in this study

contains all the results obtained; each UTS value is the average of three values.

Figure 8 depicts the mechanical properties obtained in terms of UTS for each printing strategy by the three plates having different materials adopted in this study. By using the steel plate, it can be observable an improvement in the UTS by increasing the printing speed from 70 to 110 mm/s by fixing an extrusion temperature equal to 215 °C. At the same time, the property is worsening with the same speed variation by fixing a temperature of 215/230 °C. The nimonic plate shows the same trend in terms of UTS by increasing the printing speed. Conversely, this trend is not respected with the use of the aluminum plate. In this case, by increasing the printing speed from 70 to 110 mm/s, there is an improvement in the UTS with the extrusion temperature equal to 215/230 °C, while it worsens with the increase in printing speed at 215 °C.

The results obtained fall within the value ranges demonstrated in the literature for PLA. In fact, the PLA tensile strength is typically about 40/60 MPa and that of printed PLA is about 46 MPa. Thus, a printing speed of 110 mm/s leads to better mechanical properties than a printing speed of 70 mm/s, both with a temperature of 215 °C and 215/230 °C.

Energy consumption and tensile strength have been jointly investigated to understand how FDMed PLA parts having good mechanical properties can be obtained by minimizing the energy consumption. Figure 9 shows the SEC trend over the UTS values obtained for each plate material. It can be seen that the highest values of UTS are obtained by using both steel and aluminum plates. Conversely, as far as energy consumption is concerned, aluminum has the lowest values, when compared to nimonic and steel energy consumption results.

As explained above, steel, aluminum and nimonic materials have different thermal properties. Among the three, aluminum is the material with the highest specific thermal conductivity, followed by steel and then nimonic. Since the thermal inertia, i.e., the ability of a material to oppose the passage of the heat flow and to accumulate a part of it, is indirectly proportional to the thermal conductivity, it turns out that the lowest value is typical of aluminum. A low thermal inertia results in quicker heating up of the material and a quicker transfer of heat to the environment. In fact, using aluminum and nimonic plates leads to dropping in power consumption during the printing phase (Fig. 4). The ability of aluminum to absorb heat leads to it quickly reaching the desired temperature and, therefore, stops absorbing any more energy. Instead, the nimonic retains heat as it has the highest thermal inertia, leading it to stop absorbing energy once the desired temperature is reached. On the other hand, steel is balanced in absorbing and releasing heat, as demonstrated by the trend in Figs. 4 and 5. In fact, the thermal conductivity of steel is an intermediate value between that of aluminum and nimonic. Therefore, the thermal inertia also turns out to be intermediate between the values of aluminum and nimonic.

A previous study [6] introduced a new efficiency index given by the ratio between UTS and SEC. It explains numerically how higher the tensile strength is obtained for unit-specific energy consumption in the FDM process. The index values calculated are shown in Table 4. A higher UTS/SEC value indicates a better process efficiency for that printing strategy. Figure 10 shows the variation of this efficiency index by varying the printing strategy for each plate material adopted in this study. Using the aluminum plate, the best performance in terms of tensile strength for the specific energy consumption has been observed with the strategy $V = 110$ mm/s $T = 215$ °C. Conversely, the worst case has been observed with the strategy $V = 70$ mm/s $T = 215$ °C by using the steel plate. This index confirms the results obtained in the previous comparisons.

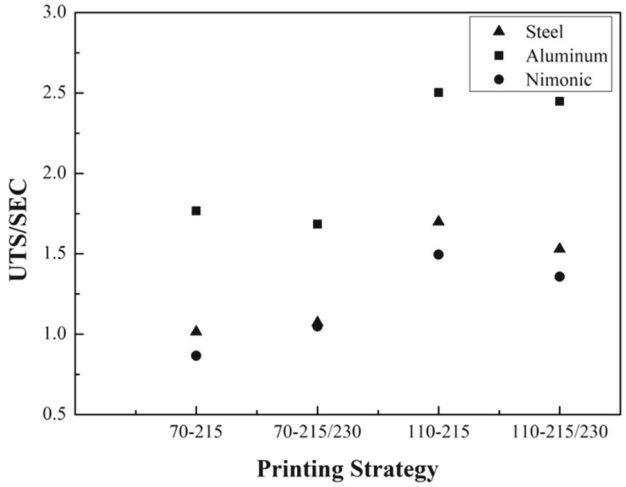

Fig. 10 UTS/SEC SEC versus the printing strategies adopted in this study

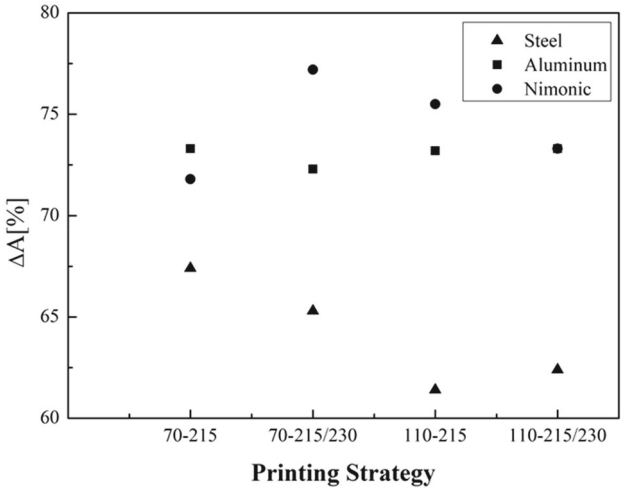

Fig. 11 Variations in the amplitude of the signal, ΔA, for all scan strategies used and for the three different printing plates adopted

3.3 Ultrasonic Inspection

Figure 11 shows the variations in the amplitude of the Ascan signal, ΔA, between the background echo and the initial one for all the temperature and speed strategies used and the three different printing plates adopted. We remember that the attenuation of the signal can be an index of compactness and homogeneity of the analyzed component. Therefore, the lower the attenuation of the input signal, the better the quality of the product, indicating the absence of manufacturing defects. However, intermediate echoes between the input and output echoes in the Ascan visual could also indicate a defect.

As you can see in the figure, the attenuation of the amplitude is lower for a strategy with a higher printing speed, indicating faster compaction of the printed sample. Compaction worsens with the increase in extrusion temperature.

Correlating ultrasound echo attenuation amplitude with two characteristic parameters of the materials' mechanical properties, UTS and SEC, it is possible to evaluate whether the product's quality affects its mechanical performance.

By analyzing the data mentioned above, the ultrasound analysis confirms greater uniformity of the material at a printing speed $V = 110$ mm/s for various printing plates adopted, similar to what is demonstrated by the mechanical properties (UTS) and energy consumption (SEC) of the process used. However, the minimum variation in ultrasound signal attenuation recorded varying the adopted strategies indicates a low influence of the printing plates used.

3.4 Overall Cost Analysis

By considering the dimensions of the bed surface, the total volume is 202.5 cm^3 and is the same for each plate employed. In order to calculate the cost of the setup, it was decided to consider the raw material cost for weight because the required machining operations are very simple and could be considered negligible compared to the price of the bulk material. In the following table (Table 6) the more relevant data useful to perform a proper cost analysis are reported.

The final cost of the nimonic bed is very high, compared to the others plates, and could be justified when the printing surfaces and the workpieces have large dimensions, then the control of distortions or temperature stability is mandatory. The costs of the steel and aluminum plates are comparable and the preference of the second one is motivated by the long term energy saving, as demonstrated in the previous evaluation.

4 Conclusions

In this study, the technological and environmental sustainability of a common FDM 3D printer for PLA components has been studied and evaluated to define a correspondence between the main FDM process conditions and the efficiency of this technology, evaluating its performance in terms of both quality and energy consumption. The effect of three printing plates having three different materials on the energy consumption in the FDM process, correlated to the quality of the parts, has been investigated. Tensile and ultrasound test specimens were printed on each plate for three temperature and print speed strategies.

All the results previously discussed lead to the following conclusions:

- All the different temperature strategies led to results comparable with the literature on FDMed PLA.

Table 6 Cost analysis for the selected bed surfaces

Bed material	Volume (cm^3)	Density (g/cm^3) [29]	Weight (kg)	Price* (€/kg)	Final bed cost (€)
Steel	202.5	7.80	1.58	0.98	1.55
Aluminum		2.78	0.56	3.50	1.96
Nimonic		8.37	1.69	17.50	29.57

*Average price obtained by consulting different producers

- The print speed strategy resulting in the best results in terms of energy consumption and mechanical properties is 110 mm/s.
- The tensile tests carried out gave results in line with expectations, as UTS values obtained are comparable to the literature.
- It is better to use aluminum plates for the desktop 3D printers rather than steel plates, as usual, to reduce power and energy consumption of the FDM process.
- Both the steel and nimonic plates led to an improvement in UTS by increasing the printing speed from 70 to 110 mm/s by fixing an extrusion temperature equal to 215 °C, while there is a worsening of the property with the same speed variation by fixing a temperature of 215/230 °C.
- The ultrasound analysis confirms greater uniformity of the material at a printing speed $V = 110$ mm/s for all the printing plates adopted, and the minimum variation in ultrasound signal attenuation recorded varying the adopted strategies indicates a low influence of the printing plates used.
- The highest UTS values were obtained using steel and aluminum plates. Conversely, as far as energy consumption is concerned, aluminum has the lowest values when compared to nimonic and steel energy consumption results.
- The best results in terms of tensile strength for the specific energy consumption (UTS/SEC) have been observed by selecting $V = 110$ mm/s and $T = 215$ °C as process conditions by using the aluminum plate. Conversely, the worst case has been observed with the strategy $V = 70$ mm/s $T = 215$ °C by using the steel plate.
- Overall cost analysis, regarding the bed production, allows to consider that two materials are more suitable for mass production of desk devices, steel and aluminum, with little preference for the second one if considered the long-term energy saving. The nimonic bed could be useful for large devices or for workpieces in which the dimensionality accuracy is priority.

This research work could be considered the start point for many other studies which are aimed to correlate the energy consumption and the mechanical properties of the printed workpieces. Other bed materials, also nonmetallic, need to be tested. Furthermore, the application of the most expensive nimonic could be implemented in large 3D printers, where the distortions or the heat dissipation are the main issues. Finally, a complete LCA, which includes also the production of the metal alloys and the manufacturing of the rolling sheets, could be extended in the future.

Acknowledgements The authors would like to gratefully thank the LabCaMP2 for the support in the experimental activities.

Author Contributions Ersilia Cozzolino: conceptualization, validation, formal analysis, investigation, data curation, writing—original draft, writing—review & editing, visualization. Francesco Napolitano: conceptualization, validation, formal analysis, investigation, data curation, writing—original draft, writing—review & editing, visualization. Ilaria Papa: conceptualization, methodology, validation, formal analysis, supervision, writing—review & editing. Antonino Squillace: methodology, validation, supervision, conceptualization, resources, project administration. Antonello Astarita: conceptualization, validation, resources, project administration, supervision.

Funding The authors declare that no funds, grants, or other support were received during the preparation of this manuscript.

Data Availability The datasets generated during and/or analyzed during the current study are available from the corresponding author on reasonable request.

Declarations

Conflict of interest On behalf of all authors, the corresponding author states that there is no conflict of interest.

References

1. Luo, Y.; Ji, Z.; Leu, M.C.; Caudill, R.: Environmental performance analysis of solid freeform fabrication processes. IEEE Int. Symp. Electron. Environ.Symp. Electron. Environ. (1999). https://doi.org/10.1109/isee.1999.765837
2. Morrow, W.R.; Qi, H.; Kim, I., et al.: Environmental aspects of laser-based and conventional tool and die manufacturing. J. Clean. Prod. **15**, 932 (2007). https://doi.org/10.1016/j.jclepro.2005.11.030
3. Niaki, M.K.; Torabi, S.A.; Nonino, F.: Why manufacturers adopt additive manufacturing technologies: the role of sustainability. J. Clean. Prod. **222**, 381–392 (2019). https://doi.org/10.1016/j.jclepro.2019.03.019
4. Tang, Y.; Mak, K.; Zhao, Y.F.: A framework to reduce product environmental impact through design optimization for additive manufacturing. J. Clean. Prod. **137**, 1560–1572 (2016). https://doi.org/10.1016/j.jclepro.2016.06.037

5. Gebler, M.; Schoot Uiterkamp, A.J.M.; Visser, C.: A global sustainability perspective on 3D printing technologies. Energy Policy **74**, 158–167 (2014). https://doi.org/10.1016/j.enpol.2014.08.033
6. Napolitano, F.; Cozzolino, E.; Papa, I., et al.: Experimental integrated approach for mechanical characteristic optimization of FDM-printed PLA in an energy-saving perspective. Int. J. Adv. Manuf. Technol. (2022). https://doi.org/10.1007/s00170-022-09535-z
7. Lalegani Dezaki, M.; Mohd Ariffin, M.K.A.; Hatami, S.: An overview of fused deposition modelling (FDM): research, development and process optimisation. Rapid Prototyp. J. **27**, 562–582 (2021). https://doi.org/10.1108/RPJ-08-2019-0230
8. Peng, X.; Zhang, M.; Guo, Z., et al.: Investigation of processing parameters on tensile performance for FDM-printed carbon fiber reinforced polyamide 6 composites. Compos. Commun. **22**, 100478 (2020). https://doi.org/10.1016/j.coco.2020.100478
9. Luzanin, O.; Movrin, D.; Stathopoulos, V., et al.: Impact of processing parameters on tensile strength, in-process crystallinity and mesostructure in FDM-fabricated PLA specimens. Rapid Prototyp. J. **25**, 1398–1410 (2019). https://doi.org/10.1108/RPJ-12-2018-0316
10. Mostafa, K.G.; Montemagno, C.; Qureshi, A.J.: Strength to cost ratio analysis of FDM nylon 12 3D printed parts. Proc. Manuf. **26**, 753–762 (2018). https://doi.org/10.1016/j.promfg.2018.07.086
11. Khabia, S.; Jain, K.K.: Comparison of mechanical properties of components 3D printed from different brand ABS filament on different FDM printers. Mater. Today Proc. **26**, 2907–2914 (2019). https://doi.org/10.1016/j.matpr.2020.02.600
12. Lay, M.; Thajudin, N.L.N.; Hamid, Z.A.A., et al.: Comparison of physical and mechanical properties of PLA, ABS and nylon 6 fabricated using fused deposition modeling and injection molding. Compos. Part B Eng. **176**, 107341 (2019). https://doi.org/10.1016/j.compositesb.2019.107341
13. Agarwal, K.M.; Shubham, P.; Bhatia, D., et al.: Analyzing the impact of print parameters on dimensional variation of ABS specimens printed using fused deposition modelling (FDM). Sens. Int. **3**, 100149 (2022). https://doi.org/10.1016/j.sintl.2021.100149
14. Choi, Y.H.; Kim, C.M.; Jeong, H.S.; Youn, J.H.: Influence of bed temperature on heat shrinkage shape error in FDM additive manufacturing of the ABS-engineering plastic. World J. Eng. Technol. **04**, 186–192 (2016). https://doi.org/10.4236/wjet.2016.43d022
15. Messimer, S.L.; Patterson, A.E.; Muna, N., et al.: Characterization and processing behavior of heated aluminum-polycarbonate composite build plates for the fdm additive manufacturing process. J. Manuf. Mater. Process. **2**, 12 (2018). https://doi.org/10.3390/jmmp2010012
16. Lepoivre, A.; Boyard, N.; Levy, A., et al.: Heat transfer and adhesion study for the FFF additive manufacturing process. Proc. Manuf. **47**, 948–955 (2021)
17. Kousiatza, C.; Chatzidai, N.; Karalekas, D.: Temperature mapping of 3D printed polymer plates: experimental and numerical study. Sensors (Switzerland) **17**, 456 (2017). https://doi.org/10.3390/s17030456
18. Vanaei, H.R.; Shirinbayan, M.; Deligant, M., et al.: In-process monitoring of temperature evolution during fused filament fabrication: a journey from numerical to experimental approaches. Thermo **1**, 332–360 (2021). https://doi.org/10.3390/thermo1030021
19. Prajapati, H.; Salvi, S.S.; Ravoori, D.; Jain, A.: Measurement of the in-plane temperature field on the build plate during polymer extrusion additive manufacturing using infrared thermometry. Polym. Test. **92**, 106866 (2020). https://doi.org/10.1016/j.polymertesting.2020.106866
20. Roy, M.; Yavari, R.; Zhou, C., et al.: Prediction and experimental validation of part thermal history in the fused filament fabrication additive manufacturing process. J. Manuf. Sci. Eng. Trans. ASME **141**, 121001 (2019). https://doi.org/10.1115/1.4045056
21. Brenken, B.; Barocio, E.; Favaloro, A., et al.: Fused filament fabrication of fiber-reinforced polymers: a review. Addit. Manuf.. Manuf. **21**, 1–16 (2018)
22. Go, J.; Schiffres, S.N.; Stevens, A.G.; Hart, A.J.: Rate limits of additive manufacturing by fused filament fabrication and guidelines for high-throughput system design. Addit. Manuf.. Manuf. **16**, 1–11 (2017). https://doi.org/10.1016/j.addma.2017.03.007
23. Dey, A.; Yodo, N.: A systematic survey of FDM process parameter optimization and their influence on part characteristics. J. Manuf. Mater. Process. **3**, 64 (2019). https://doi.org/10.3390/jmmp3030064
24. Wang, L.; Gramlich, W.M.; Gardner, D.J.: Improving the impact strength of Poly(lactic acid) (PLA) in fused layer modeling (FLM). Polymer (Guildf) **114**, 242–248 (2017). https://doi.org/10.1016/j.polymer.2017.03.011
25. Tsouknidas, A.; Pantazopoulos, M.; Katsoulis, I., et al.: Impact absorption capacity of 3D-printed components fabricated by fused deposition modelling. Mater. Des. **102**, 41–44 (2016). https://doi.org/10.1016/j.matdes.2016.03.154
26. Moradi, M.; Meiabadi, S.; Kaplan, A.: 3D printed parts with honeycomb internal pattern by fused deposition modelling; experimental characterization and production optimization. Met. Mater. Int.. Mater. Int. **25**, 1312–1325 (2019). https://doi.org/10.1007/s12540-019-00272-9
27. Lawrence, A.; Thollander, P.; Andrei, M.; Karlsson, M.: Specific energy consumption/use (SEC) in energy management for improving energy efficiency in industry: meaning, usage and differences. Energies **12**, 247 (2019). https://doi.org/10.3390/en12020247
28. ASTM-D638-14 (2014) Standard test method for tensile properties of plastics. ASTM Stand
29. MatWeb - material property data. https://www.matweb.com/index.aspx